AD-A088 336 NEW MEXICO STATE UNIV LAS CRUCES DEPT OF PHYSICS F/G 4/1
ATMOSPHERIC EXTINCTION MODEL MODIFICATION ANALYSIS.(U)
SEP 79 A MILLER, E BURLBAW DAAD07-79-M-6275
UNCLASSIFIED NL

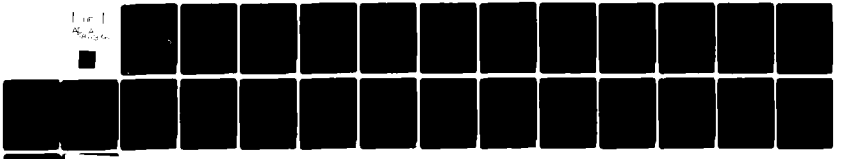

END
DATE FILMED
10-80
DTIC

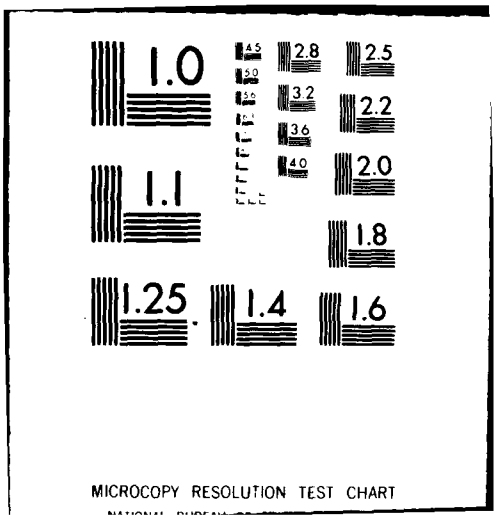
1.0
1.1
1.25
1.4
1.6
1.8
2.0
2.2
2.5
2.8
3.2
3.6
4.0
4.5
5.0
5.6
MICROCOPY RESOLUTION TEST CHART

LEVEL II

FINAL REPORT

Contract DAAD07-79-M-6275

ATMOSPHERIC EXTINCTION MODEL MODIFICATION ANALYSIS

Prepared by

August Miller and Edward Burlbaw
Department of Physics
New Mexico State University
Las Cruces, NM 88003

September 1979

This document summarizes modifications of ASL supplied atmospheric extinction models carried out at NMSU under Contract DAAD07-79-M-6275. The particular modifications which have been examined and completed are the following:

(1) Revision of the line-by-line model (ATRAN) to include an additional line-profile (the 'Gross' profile) for use at near-millimeter wavelengths,

(2) Revision of the single-scattering aerosol code AGAUSX to provide for user supplied inputs and program outputs describing the polarization properties of incident and scattered radiation,

(3) Development and demonstration of a code for calculating, tabulating and plotting the results of Mie calculations using those WSMR facilities which are routinely available to ASL,

(4) Adaptation of an ASL supplied "continued fraction" approach to Bessel function calculations as a substitute for the forward recursion methods previously employed by subroutine MIEGX in program AGAUSX, AND

(5) Further examination of the effects of relative humidity on extinction by hygroscopic aerosols using an FS smoke model.

The topics and results listed above are discussed in more detail below.

High-Resolution Model Modifications

The ASL line-by-line transmittance modeling code ATRAN has been revised to provide users the option of choosing a line shape which may be more appropriate at submillimeter wavelengths than those line shapes

previously encoded. The particular line profile which has been added is the normalized Gross profile*:

$$\phi(\nu) = \frac{\nu^2}{(\nu_o^2 - \nu^2)^2 + 4\alpha^2\nu^2} \cdot \left(\frac{4\alpha}{\pi}\right) ,$$

where α is the half-width at half-maximum of an absorption centered at wavenumber ν_o.

Inclusion of this line profile (which is selected by setting input parameter IPRO equal to 6), required modification of the main program (ATRAN14), and subroutine HTRN13. The modified versions have been designated ATRAN15 and HTRN15, respectively, and copies of the revised versions will be delivered separately. Results of sample runs comparing the choice of the Gross profile and the Lorentz profile are shown in Figure 1.

Single-Scattering Aerosol Model Modifications

1. Program AGAUSX has been revised so as to include calculation and printout of quantities describing the polarization properties of scattered radiation. The addition of these capabilities requires that the user provide a new input data card containing information describing the "Modified" Stokes parameters of the incident radiation. Those four parameters are usually represented by the symbols {I_1,I_2,U, and V}. The

*E. P. Gross, Phys. Rev. 97, 395 (1955).

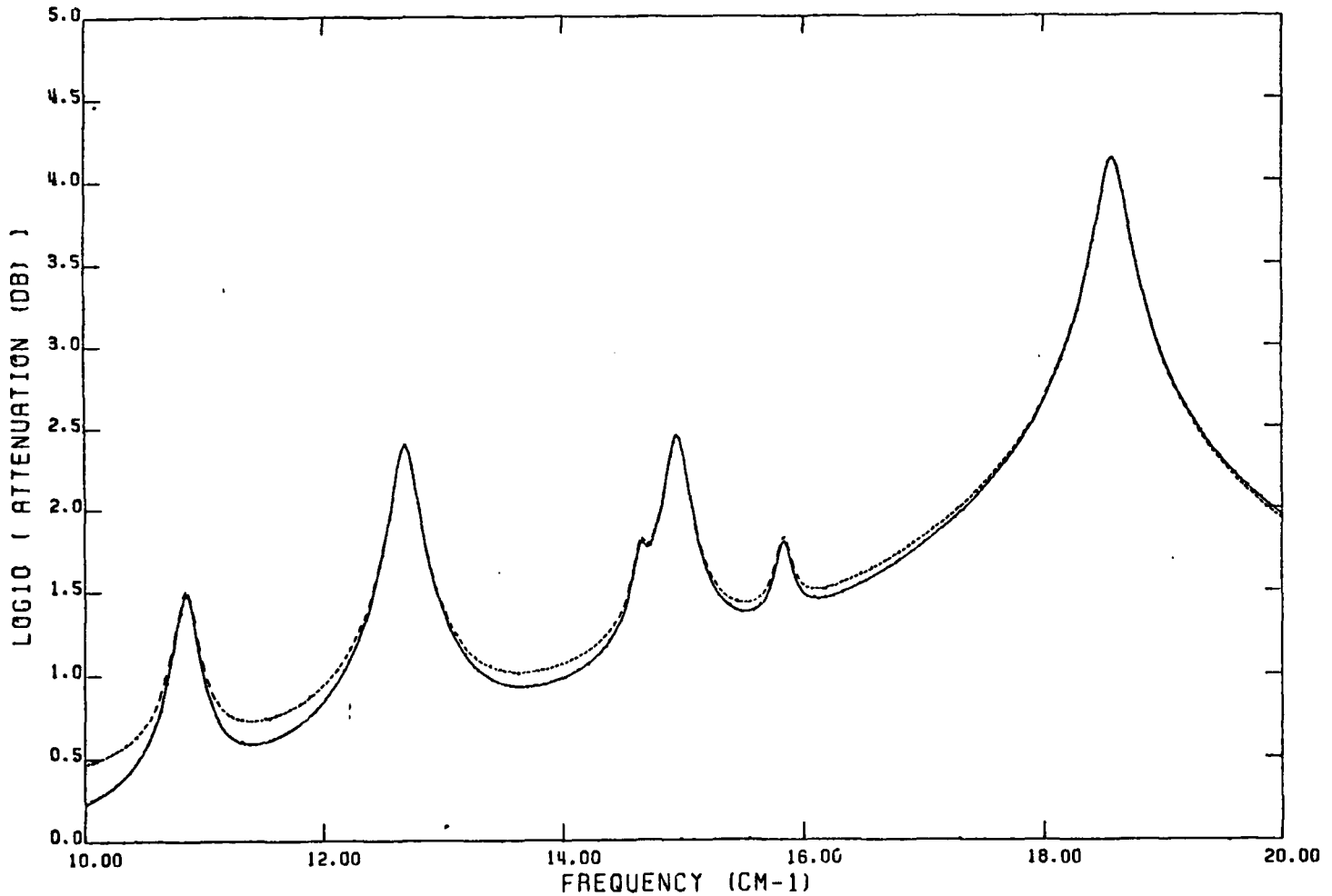

Figure 1. Comparison of attenuation over a 1 km sea-level path at near-millimeter wavelengths for Gross (solid line) and Lorentz (dashed line) profiles; computations were performed at increments of 0.02 cm^{-1} using a modified version of program ATRAN.

forms used in the revision of AGAUSX are consistent with those found in the RRA code MIE2. Explicitly, if one defines four "intensities" $i_j(\theta)$ from the Mie amplitude functions $S_1(\theta)$ and $S_2(\theta)$ as follows:

$$i_1(\theta) = |S_1(\theta)|^2 ,$$

$$i_2(\theta) = |S_2(\theta)|^2 ,$$

$$i_3(\theta) = \mathrm{Re}\{S_1(\theta)S_2^*(\theta)\} \equiv \sqrt{i_1 i_2}\cos\delta ,$$

$$i_4(\theta) = -\mathrm{Im}\{S_1(\theta)S_2^*(\theta)\} \equiv -\sqrt{i_1 i_2}\sin\delta ,$$

then, the modified Stokes parameters, after scattering, are given (to within a normalization factor) by:

$$I_1(\theta) = i_1(\theta)I_{10}$$

$$I_2(\theta) = i_2(\theta)I_{20}$$

$$U(\theta) = i_3(\theta)U_0 + i_4(\theta)V_0$$

$$V(\theta) = i_3(\theta)V_0 - i_4(\theta)U_0 ,$$

where subscript "zero" refers to the incident radiation.

The sum of parameters $I_1(\theta)$ and $I_2(\theta)$ is, except (again) for a normalization factor, identical to the "phase function" already calculated in AGAUSX. In the revised code the four Stokes parameters have been given the same normalization as the phase function, namely,

$$\int I_1(\theta)d\Omega + \int I_2(\theta)d\Omega = 4\pi\tilde{\omega}_0 \ ,$$

or,
$$I_1(\theta) + I_2(\theta) = P(\theta),$$

where $P(\theta)$ is the phase function found in AGAUSX. The normalization factor is $\lambda^2/(\pi C_{ext})$, where C_{ext} is the extinction cross-section averaged over particle sizes.

In the above symbols, I_1 is the intensity of the component of the electric field perpendicular to the plane of scattering, and I_2 is that parallel to the same plane. If one defines two parameters Q and W as follows:

$$Q(\theta) \equiv I_1(\theta) - I_2(\theta),$$

and,
$$W(\theta) \equiv \left[Q^2(\theta) + U^2(\theta) + V^2(\theta)\right]^{\frac{1}{2}} \ ,$$

then the "degree of polarization" is defined to be:

$$DOP(\theta) = 100 \times \left(\frac{W(\theta)}{I_1(\theta) + I_2(\theta)}\right) \qquad [\text{percent}] \ ,$$

and the "ellipticity" is taken to be

$$\varepsilon(\theta) = \frac{V(\theta)}{W(\theta) + \left[Q^2(\theta) + U^2(\theta)\right]^{\frac{1}{2}}} \ .$$

A third parameter of interest is:

$$\chi(\theta) = 0.5 \arctan U/Q.$$

Detailed discussions of the modified Stokes parameters can be found in the book Electromagnetic Scattering on Spherical Polydispersions, by D. Diermendjian.

The revised version of AGAUSX, which will be called AGAUSXP, requires that the user provide input values for $\{I_{10}, I_{20}, U_0$, and $V_0\}$, and provides printouts of (a) the degree of polarization, (b) the ellipticity, and (c) the four quantities $\{I_1, I_2, U$ and $V\}$ at angles determined by input parameters "IT" and "IANG".

The input Stokes parameters are read by AGAUSXP main on a new card 1.5 (i.e., between cards 1 and 2). Examples of input Stokes parameters follow:

Natural light, (0.5,0.5,0.0,0.0); linearly polarized parallel or perpendicular to scattering plane ($\chi_0 = 0$ or ± 90), (1.0,0.0,0.0,0.0) or (0.0,1.0,0.0,0.0); linearly polarized with $\chi_0 = 45°$ (0.5,0.5,1.0,0.0) and circularly polarized (0.5,0.5,0.0,1.0). χ_0 is defined as the angle between the main axis of the polarization ellipse and the plane of observation.

Comparison runs using Radiation Research Associates' Mie routine MIE2 and AGAUSXP agreed, with the exception of the normalization constants.

Table 1. Partial printout from AGAUSXP

Polarization, Ellipticity, and Scattered Stokes Vector is for incident Stokes Vector: (.50, .50, .00, .00)

Angle	Polarization	Ellipticity	Scattered Stokes Vector
.00	.0000000	.00000	(1.43+003,1.43+003,.00,.00)
45.00	67.1644659	.00000	(9.86-002,1.94-002,.00,.00)
90.00	72.3145247	.00000	(4.00-002,6.43-003,.00,.00)
135.00	20.6919627	.00000	(2.23-002,1.47-002,.00,.00)
180.00	.0000000	.00000	(1.84-002,1.84-002,.00,.00)

2. The next section describes a set of programs and procedures which may be used to calculate, print (in tabular form) and plot the extinction, scattering, and absorption efficiencies (Q_{ext}, Q_{sca},Q_{abs}) for a range of Mie size parameters, α. The tables are in an 8½ x 11-inch format allowing 1½-inch left margin and 1-inch right margin (Table 2). The plots are scaled to allow similar margins (Fig. 2).

Program WAVQ reads input data (up to 10 sets) for wavelength (in micrometers) and the real and imaginary parts of the index of refraction: Y, EM, CA (3F8.5). It then calculates the Mie absorption, extinction and scattering efficiency factors: QAB, QEX, QSC, respectively, for the range of Mie size parameter, α, from 0.1 to 20.0 by 0.1 increments and writes them into an external data file defined as unit No. 1.

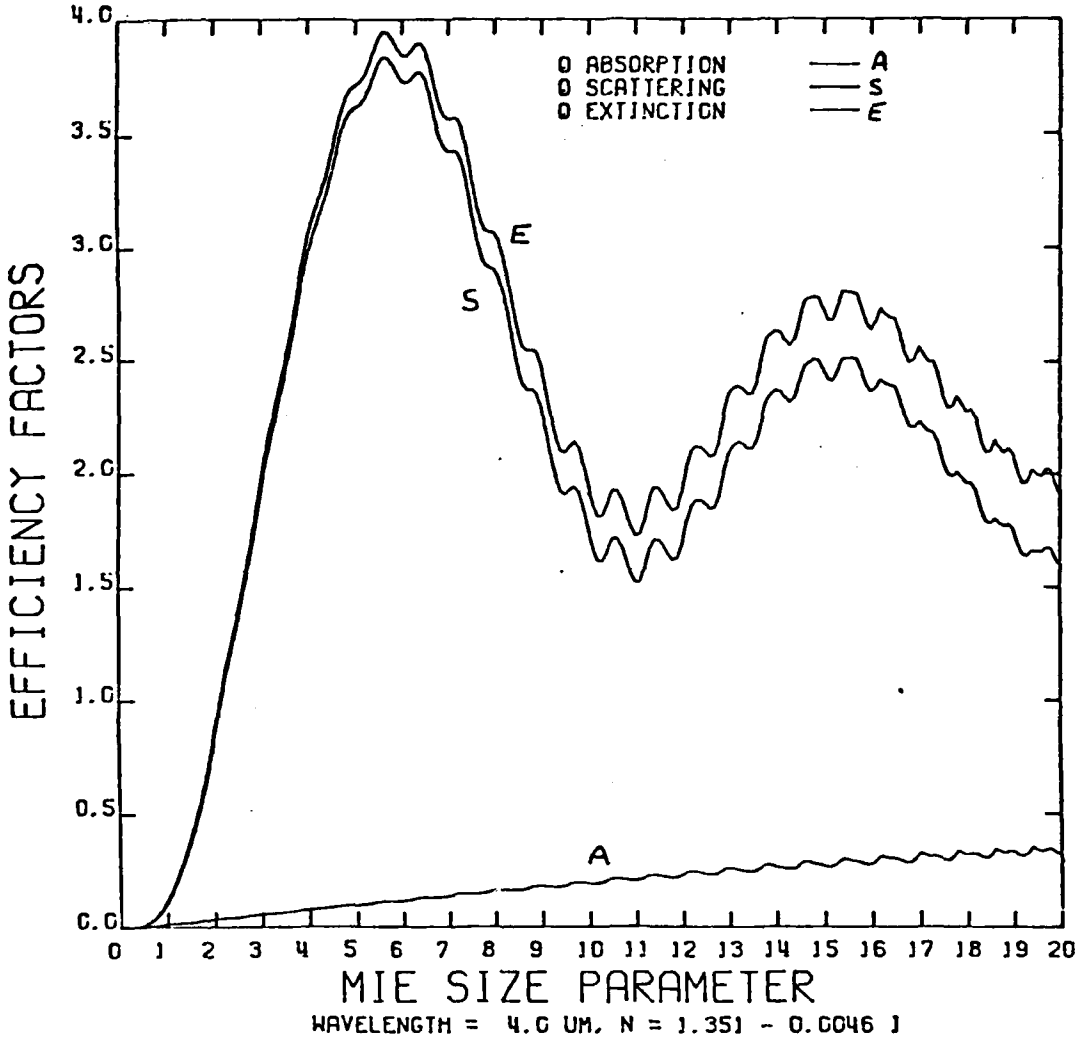

Figure 2. Sample plot generated using Program QPLOT.

A simplified flow chart of WAVQ is shown below:

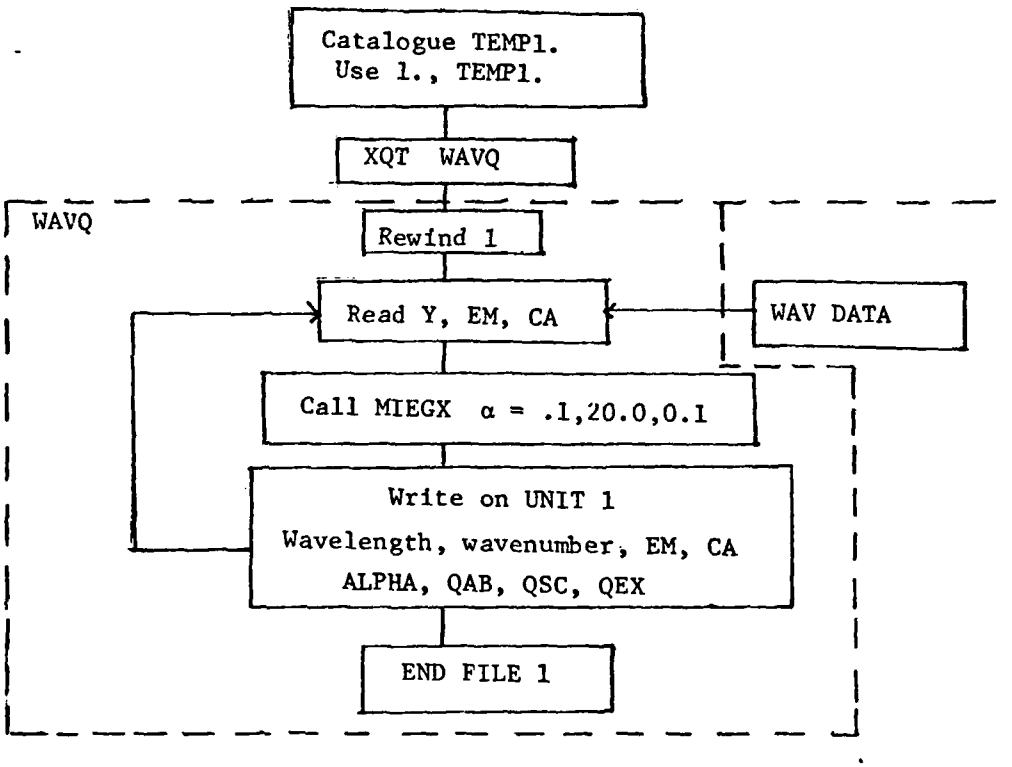

An equivalent program for the GHz region, GHZQ, reads input values of frequency (in GHz), real and imaginazy parts of the index of refraction: F, EM, CA (3F8.5). This program, however, writes on unit #2 which must be a previously assigned and catalogued file.

Program RNWWAV reads from the data file (unit #1) and prints in tabular form the Q's versus alpha for each set of wavelength (micrometers) M, K. It is suggested that the forms control option for reversed paper

Table 2. Sample Output of Program RNWWAV

WAVELENGTH (MICROMETERS): 4.00
WAVENUMBER (INVERSE CM.): 2500.0
INDEX OF REFRACTION: 1.351 - .00460 I

ALPHA	Q ABSORPTION	Q SCATTERING	Q EXTINCTION
.1	1.02339-003	1.24055-005	1.03580-003
.2	2.07090-003	1.98130-004	2.26904-003
.3	3.16543-003	9.99642-004	4.16508-003
.4	4.32741-003	3.14184-003	7.46924-003
.5	5.57334-003	7.60484-003	1.31782-002
.6	6.91420-003	1.55691-002	2.24833-002
.7	8.35377-003	2.83171-002	3.66709-002
.8	9.88749-003	4.70781-002	5.69656-002
.9	1.15026-002	7.28169-002	8.43196-002
1.0	1.31810-002	1.06000-001	1.19181-001
1.1	1.49050-002	1.46420-001	1.61325-001
1.2	1.66667-002	1.93210-001	2.09876-001
1.3	1.84784-002	2.45147-001	2.63625-001
1.4	2.03778-002	3.01278-001	3.21656-001
1.5	2.24238-002	3.61679-001	3.84103-001
1.6	2.46775-002	4.28004-001	4.52681-001
1.7	2.71677-002	5.03380-001	5.30548-001
1.8	2.98501-002	5.91264-001	6.21114-001
1.9	3.25832-002	6.93287-001	7.25870-001
2.0	3.51526-002	8.07039-001	8.42192-001
2.1	3.73647-002	9.25674-001	9.63039-001
2.2	3.91632-002	1.04066+000	1.07982+000
2.3	4.06807-002	1.14626+000	1.18694+000
2.4	4.21803-002	1.24244+000	1.28462+000
2.5	4.39358-002	1.33449+000	1.37842+000
2.6	4.61226-002	1.43042+000	1.47654+000
2.7	4.87443-002	1.53754+000	1.58628+000
2.8	5.16087-002	1.65896+000	1.71057+000
2.9	5.43855-002	1.79102+000	1.84541+000
3.0	5.67669-002	1.92404+000	1.98081+000
3.1	5.86513-002	2.04736+000	2.10601+000
3.2	6.01984-002	2.15543+000	2.21563+000
3.3	6.17222-002	2.25026+000	2.31198+000
3.4	6.35275-002	2.33952+000	2.40304+000
3.5	6.57841-002	2.43274+000	2.49852+000
3.6	6.84426-002	2.53710+000	2.60555+000
3.7	7.12106-002	2.65320+000	2.72441+000
3.8	7.36090-002	2.77299+000	2.84666+000
3.9	7.55436-002	2.88349+000	2.95904+000
4.0	7.69275-002	2.97520+000	3.05213+000

(unlined side) be used. Table 2 is a sample of the printout from this program.

The associated program RNWGHZ for GHZ region varies from RNWWAV in that it reads from UNIT 2 and has the table head changed appropriately.

Program QPLOT (which calls PHPLOT and associated subroutines) reads from UNIT 1 and UNIT 2 and plots on a tape (either user supplied or contractor) the efficiency factors versus alpha. This tape must then be sent to T5 (Bldg 1623) which is usually done by console personnel when the tape is freed. The user must then go to T5 and complete an Operations Work Request card supplying such information as TAPE ID, number of plots on tape and width of paper required; in this case 12-inch paper is required. As programmed the plots are approximately 6"x6". The size can be easily changed by changing variable FACT in QPLOT following instructions in PHPLOT comments. For the sake of clarity the three curves on each plot were given the same symbol so it will be necessary for the user to identify the curves appropriately using the tables printed by RNWWAV and GHZWAV.

Because QPLOT (as supplied) plots both the micrometer and GHZ plots on the same tape it is necessary to supply plotting data elements to the PHPLOT subroutine (called WAVPD and GHZPD in supplied listing). The plotting data elements determine the headings to be printed on the plots and must be supplied by the user in the right order so that the correct headings appear on the corresponding plots generated from the data read. Of course, WAVPD and GHZPD must be modified if different sets of refractive indices and wavelength are used. The format of the data is described in the comment section of PHPLOT. PHPLOT and its associated subroutines

was developed by Dr. Richard Shirkey now at the Atmospheric Sciences Laboratory.

The described set of programs are presently set up to calculate, print and plot the efficiency factors vs. alpha for 10 different wavelengths in the micrometer region and 7 different frequencies in the GHZ region and can easily be modified by someone familiar with Fortran. The crucial statements are the DO statements in WAVQ and GHZQ for reading the data cards, the corresponding DO statements in RNWWAV and RNNGHZ, and the DO statements in QPLOT. The range of Mie sizes could also be changed but would require additional changes in QPLOT.

A simplified flowchart of the entire procedure as well as a sample runstream from start to finish (file RUNSTREAM) is appended.

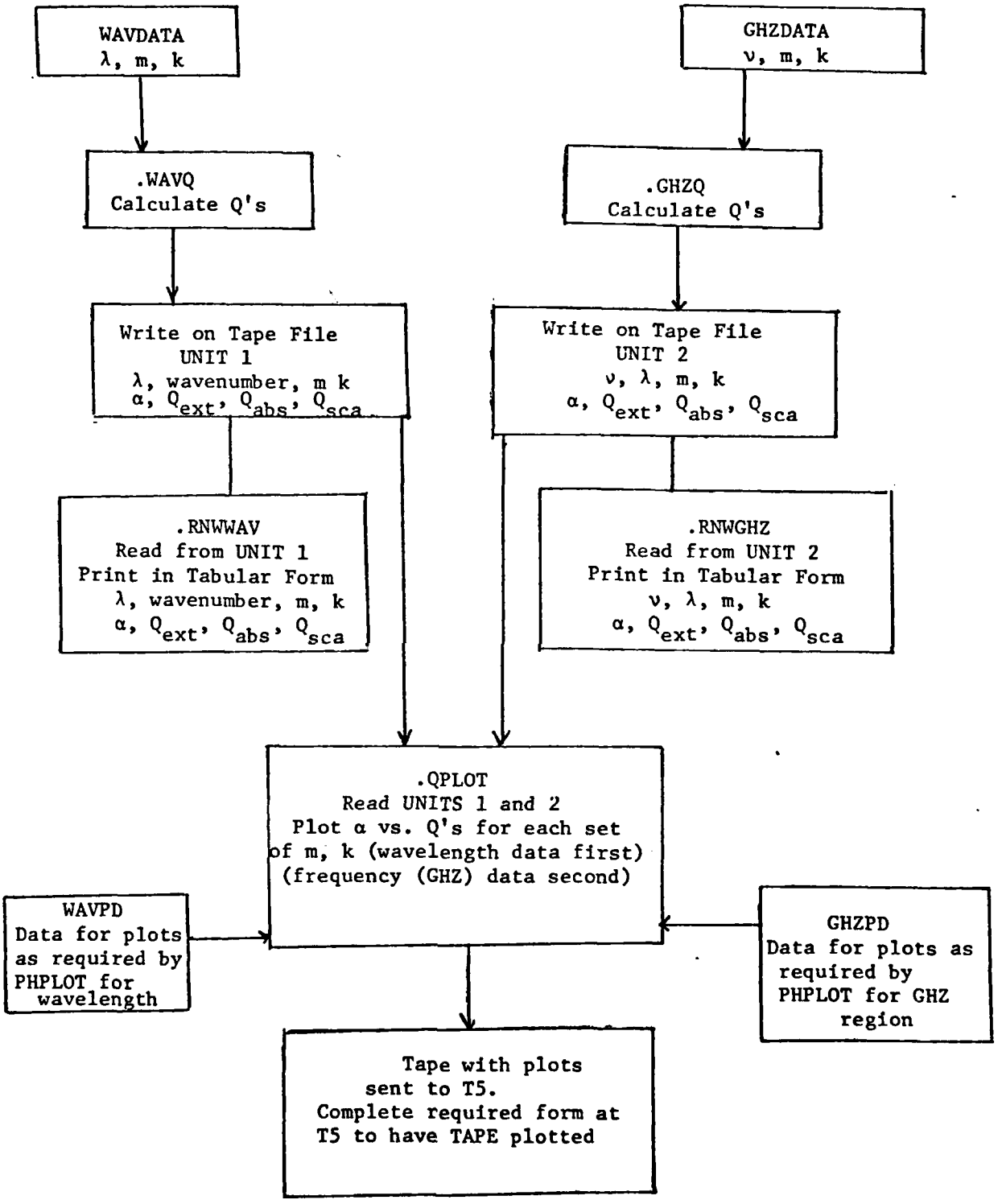
WAVDATA
λ, m, k
GHZDATA
ν, m, k
.WAVQ
Calculate Q's
.GHZQ
Calculate Q's
Write on Tape File
UNIT 1
λ, wavenumber, m k
α, Q_ext, Q_abs, Q_sca
Write on Tape File
UNIT 2
ν, λ, m, k
α, Q_ext, Q_abs, Q_sca
.RNWWAV
Read from UNIT 1
Print in Tabular Form
λ, wavenumber, m, k
α, Q_ext, Q_abs, Q_sca
.RNWGHZ
Read from UNIT 2
Print in Tabular Form
ν, λ, m, k
α, Q_ext, Q_abs, Q_sca
.QPLOT
Read UNITS 1 and 2
Plot α vs. Q's for each set
of m, k (wavelength data first)
(frequency (GHZ) data second)
WAVPD
Data for plots
as required by
PHPLOT for
wavelength
GHZPD
Data for plots as
required by
PHPLOT for GHZ
region
Tape with plots
sent to T5.
Complete required form at
T5 to have TAPE plotted

Runstream for Tabulation and Plotting Tape Generation

```
@ASG,T TAPE.,8C,C0101U
@MSG,W PAN=****,NAME=*******
@USE 23.,TAPE.
@ASG,CP TEMP1.
@ASG,CP TEMP2.
@USE 1.,TEMP1.
@USE 2.,TEMP2.
@FOR,I     .WAVQ
     .
  WAVQ DECK
     .
@FOR,I     .GHZQ
     .
  GHZQ DECK
     .
@FOR,I     .MIEGX
     .
  MIEGX DECK
     .
@FOR,I     .RNWWAV
     .
  RNWWAV DECK
     .
@FOR,I     .RNWGHZ
     .
  RNWGHZ DECK
     .
@FOR,I     .QPLOT
     .
  QPLOT DECK
     .
@FOR,I     .PHPLOT
     .
  PHPLOT DECK
     .
@FOR,I     .BOX
     .
  BOX DECK
     .
@FOR,I     .LOG
     .
  LOG DECK
     .
@FOR,I     .LETR
     .
  LETR DECK
     .
@FOR,I     .RESET
     .
  RESET DECK
     .
@FOR,I     .SETUP
     .
  SETUP DECK
     .
```

```
@FOR,I     .EXHEAD
    .
  EXHEAD DECK
    .
@ELT,I     .WAVPD
    .
  WAVPD DECK
    .
@ELT,I     .GHZPD
    .
  GHZPD DECK
    .
@MAP
IN      .WAVQ
IN      .MIEGX
END
@XQT
@ADD      .WAVDATA
@MAP
IN      .GHZQ
IN      .MIEGX
END
@XQT
@ADD      .GHZDATA
@MAP
IN      .RNWWAV
END
@XQT
@MAP
IN      .RNWGHZ
END
@XQT
@MAP,I
IN      .PHPLOT,.BOX,.LOG,.LETR,.RESET,.SETUP,.EXHEAD
IN      .QPLOT
LIB ASL*DP8PLOT
END
@XQT
@ADD      .WAVPD
@ADD      .GHZPD
@FREE TAPE
@MSG,W PLEASE DELIVER TAPE ***** TO T5
```

@ELT,I . WAVDATA
WAVDATA DECK
@ELT,I .GHZDATA
GHZDATA DECK

3. A Mie-type routine utilizing a continued fractions method of calculation was obtained from W. J. Lentz of Atmospheric Science Laboratory and modified slightly to substitute directly for MIEGX in AGAUSX. Runs calculating the efficienty factors Q_{ext} and Q_{sca} were done for comparison purposes using JLMIE, MIEGX and a routine written by Radiation Research Associates, MIE2. The three routines were found to agree for a wide range of Mie size parameter, α, when the imaginary part of the index of refraction was zero. When the imaginary part of the index became larger (on the order of 1/2 the real part) MIEGX began to give results that deviated from the JLMIE and MIE2 results for α greater than about 80, whereas, JLMIE and MIE2 results agreed for all cases for which MIE2 is considered reliable.

The comparison process was done mainly to verify that coding errors had been eliminated and was not as extensive as the comparisons given in the final report on Contract DAAD07-78-C-0063 (December 1978). However, the shortcomings of the MIEGX code were found to be consistent with those reported in that report (pages 20-30).

Table 3 shows the values of Q_{ext} and Q_{sca} calculated by each of the three routines for a selected case. The table also contains the CPU times as determined using a system supplied timing routine for each case of m, k, and α. As is obvious from the table JLMIE required approximately twice as much computing time as MIEGX and slightly less time than MIE2. One probable cause of the longer CPU times required by JLMIE and MIE2 is that both routines require complex arithmetic whereas MIEGX separates the real and imaginary parts of the calculations. A similar treatment

Table 3. Comparison of JLMIE with MIEGX and MIE2

Index of Refraction: 1.2 - 0.6i

		$Q_{scattering}$	$Q_{extinction}$	CPU Time (sec)
	MIEGX	1.20735+00	2.14598+00	0.213
$\alpha = 40$	JLMIE	1.20735+00	2.14598+00	0.402
	MIE2	1.20735+00	2.14598+00	0.478
$\alpha = 80$	MIEGX	1.19760+00	2.09627+00	0.384
	JLMIE	1.19760+00	2.09627+00	0.801
	MIE2	1.19760+00	2.09627+00	0.961
$\alpha = 100$	MIEGX	1.19442+00	2.07694+00	0.463
	JLMIE	1.19399+00	2.08388+00	0.907
	MIE2	1.19399+00	2.08388+00	1.056
$\alpha = 300$	MIEGX	9.93771+00	2.01371+00	1.314
	JLMIE	1.17761+00	2.04187+00	2.513
	MIE2	1.17761+00	2.04187+00	3.143

of JLMIE might be a worthwhile project at a future date if the length of calculation time becomes critical.

JLMIE was used for various test cases of α, m, and k including on run m = k = 5.0 for α as large as 3000 without termination by the routine itself.

The authors know of no other Mie type routine on-line at ASL that is either valid or runs for such cases and is thus usable for validation of JLMIE. Table 4 shows Q_{sca} and Q_{ext} for m = k = 5.0, α = 10 to 3000.

A comparison of the Q_{radar}'s calculated by the three codes shows at least some disagreement in all cases. The coding in JLMIE for the calculation of Q_{radar} is identical to that in MIEGX so the disagreement must be as a result of differences in the Bessel function calculations. This was not investigated under this contract but a table showing the results for Q_{radar} is included (Table 5).

From this discussion of JLMIE it can be concluded that the routine seems immune to termination on the machine level for a wide range of alpha and index of refraction. Where the computation time is not critical JLMIE would be the routine to use especially if large Mie sizes or large indices of refraction would be used.

Table 4. JLMIE results for large α and large index of refraction

Index of Refraction: 5.0 - 5.0i

α	Q_{sca}	Q_{ext}	CPU time (sec)
10	1.83974	2.33745	0.29
100	1.70745	2.10905	2.44
300	1.68047	2.05927	3.46
1000	1.66537	2.02623	8.91
2000	1.65945	2.01538	16.03
3000	1.65946	2.01339	23.54

Table 5. Comparison of Q_{radar} for JLMIE, MIEGX and RRA-MIE2

Index of Refraction: 1.2 - 0.6i

α	MIEGX	JLMIE	MIE2
35	7.69334-002	7.69337-002	7.69337-002
60	7.69292-002	7.69286-002	7.69291-002
85	7.73410-002	7.69253-002	7.69266-002
110	6.58217+000	7.69259-002	7.69252-002

Effects of Relative Humidity on Extinction at Several Wavelengths

Introduction: Two previous documents generated at NMSU (Miller, et al., 1977, and Miller, et al., 1978) contained some discussion of the effects of relative humidity on two postulated models for WP smoke. Similar calculations were made recently for an FS smoke model using parameters given by Hanel (1978). Average growth factors $\bar{\mu}(f)$ were derived from Hanel's data under the assumption that the growth of particles for any dry radii could be adequately represented by that of a particle whose dry radius was 10μm, and the optical constants were taken directly from Hanel. In lieu of better information, the initial (dry) particle distribution was chosen to be the same as used in the earlier WP models. The new computations were performed at wavelengths of 0.55, 1.06, 3.8 and 10.6μm for relative humidities of 40, 60, 70, 80, 90, 95 and 99%. The ASL single-scattering code AGAUSX was used for all computations.

Results: Figure 3 is a graph of the calculated extinction cross-sections in units of square meters per milligram of source material. These cross-sections were calculated by including the effects of absorbed liquid water in the extinction calculations but not in determination of aerosol mass. Thus, the results shown in figure 3 represent calculated extinction per unit mass of "dry" (or ordnance) material. Consequently, they directly illustrate the changes in extinction which might be expected when a given mass of smoke material is deployed under various conditions of relative humidity.

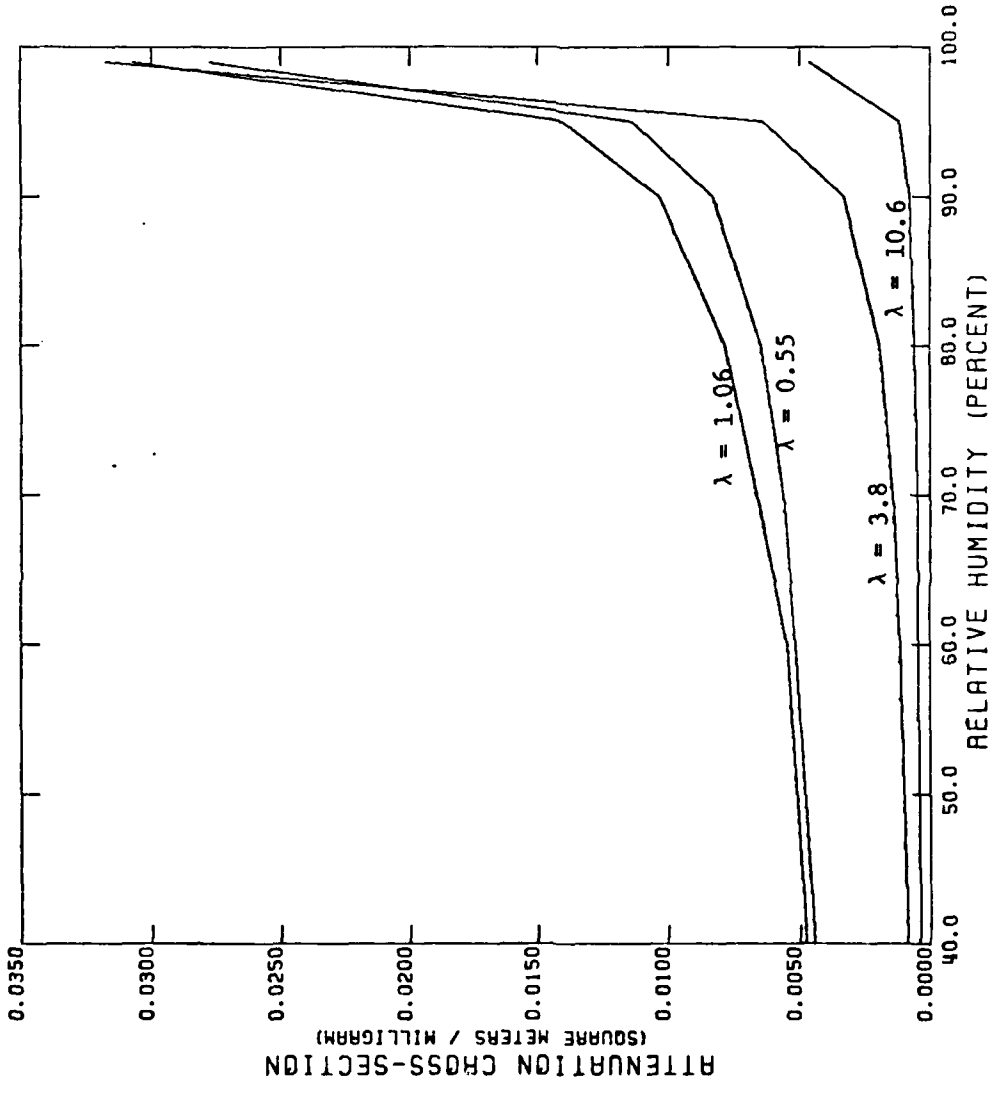

Figure 3. Attenuation cross-sections per mg of dry aerosol material for an FS smoke model at several wavelengths and relative humidities.

Figure 4 contains graphs of the ratios of the extinction cross-sections at 0.55μm to those at the other three wavelengths. If "visibility" were related to extinction cross-section at the other wavelengths in the same way as at 0.55μm, then the graphs in figure 4 would represent the way in which the "visibility ratios" would change with relative humidity for the FS smoke model. That is, under the above assumption, the curves $C_{0.55}/C_{3.8}$, for example, in figure 4 could be interpreted as representing the ratio of the visibility at 3.8μm to that at 0.55μm.

Finally, figure 5 contains graphs of the extinction cross-sections per unit mass of ambient aerosol material (source plus accreted water). It should be noted that these curves behave quite differently than those in figure 2. The data contained in figure 5 are more representative of the kinds of results to be expected from field measurements which do not distinguish between source materials and accreted water when mass determinations are made.

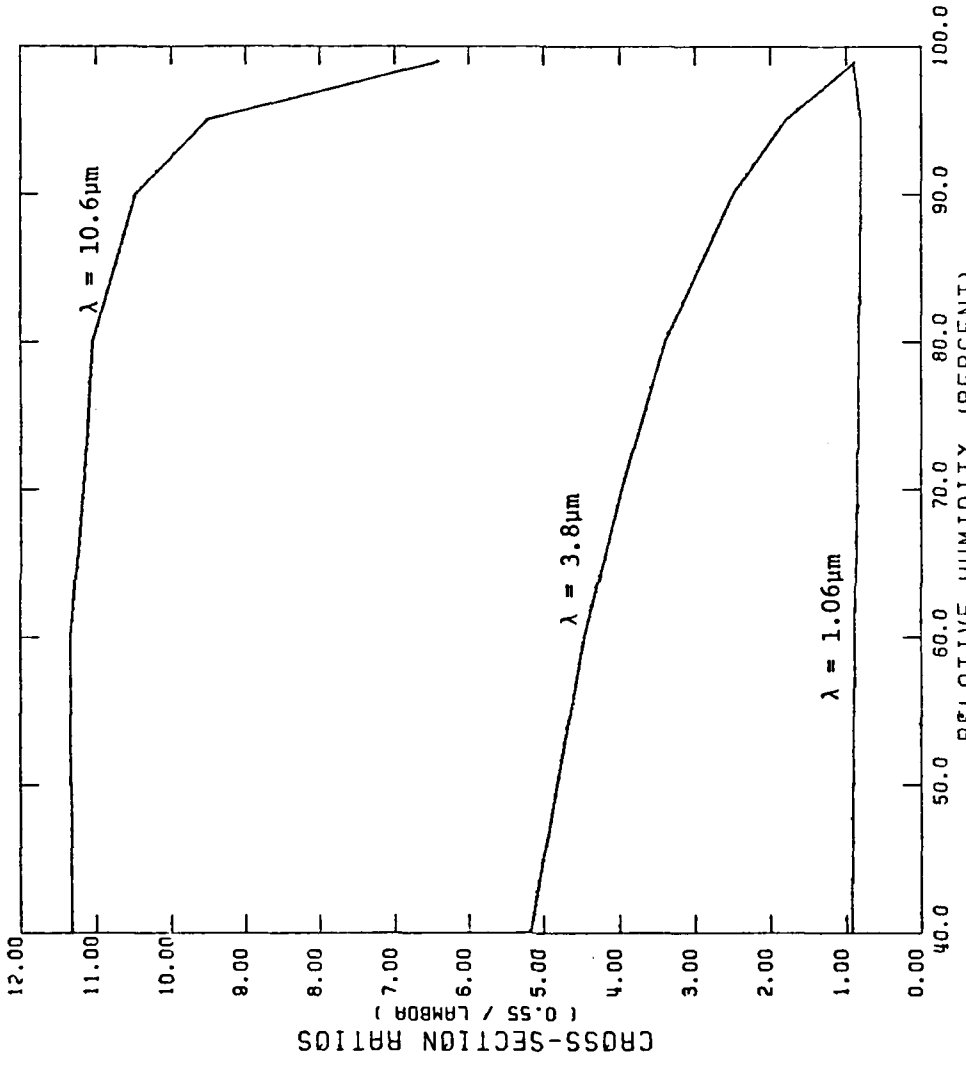

Figure 4. Ratios of attenuation cross-sections at λ = 0.55μm to those at three other wavelengths for an FS smoke model at various relative humidities.

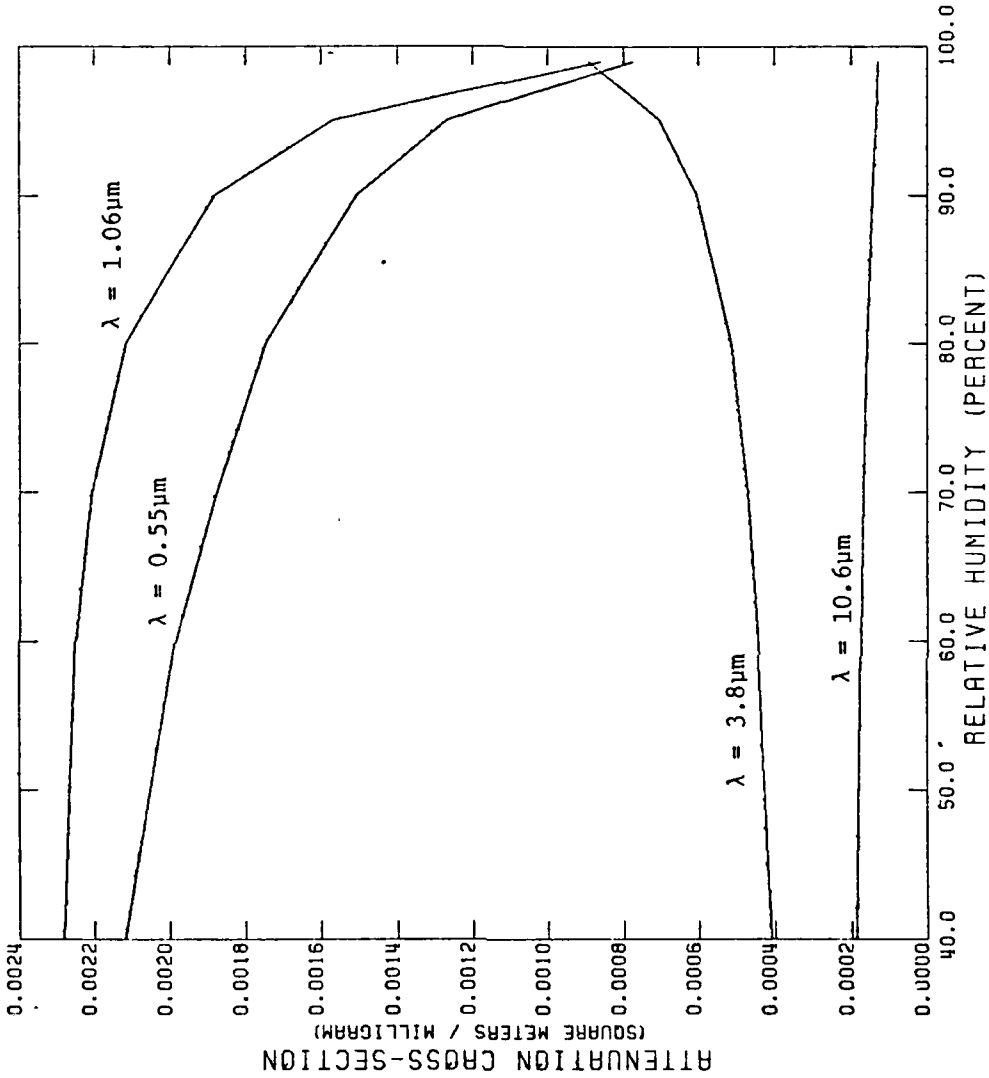

Figure 5. Attenuation cross-sections per mg of wet aerosol material for an FS smoke model at several wavelengths and relative humidities.

Other References

1. J. T. Hall, Appl. Optics 9, 1488 (1970).

2. G. Hanel, unpublished report of work done at ASL/WSMR during the period 28 Aug 1978 through 26 Sept 1978.